HYDRODYNAMIC PARTICLE TRANSPORT IN SILICA SCALE DEPOSITION

P. Kokhanenko [1], K. Brown [2] and M. Jermy [1]

[1] University of Canterbury, Department of Mechanical Engineering, Private Bag 4800, Christchurch 8041, New Zealand

[2] GEOKEM, P.O. Box 30-125, St Martins, Christchurch, New Zealand

pavlo.kokhanenko@pg.canterbuty.ac.nz

Keywords: *silica scale, colloidal silica, hydrodynamic effects, colloids stability.*

ABSTRACT

Silica scaling limits the flow rate of the geothermal fluid passing through a powerplant and hence heat and the power that can be extracted from it. The chemical kinetics of silica colloid nucleation and growth are reasonably well understood, but the hydrodynamic transport and the process of binding to solid surfaces are not. A key question is whether the rate at which particles accumulate on the surface is limited by the rate of transport of particles through the fluid near the wall, or by the fraction of particles which form permanent bonds at the surface.

Previous work by Dunstall, Zipfel and Brown showed the scale deposited on a cylindrical object placed in flowing geothermal brine varied in thickness from place to place, with thicker deposits forming in the locations where the shear stress is high. This suggests a transport-limited process.

This paper reports new computational fluid dynamics (CFD) study which suggests that if electrostatic interactions are ignored, the rate of arrival of silica particles at the surface is several orders of magnitude higher than the observed scaling rate. This suggests only a small fraction (~1 in 10^5) of the particles arriving at the wall in that experiment actually attach to it, and that the scaling process is limited by the process of bonding with the surface.

In an attempt to resolve this contradiction, the theory or particle transport and interaction has been explored. When the wall is coated with silica, colloids in motion near the wall experience electrostatic repulsion. The resultant energy barrier can be calculated from the Derjaguin, Landau, Verwey and Overbeek (DLVO) theory. It is used here to find the stability of a colloidal system under various hydrodynamic conditions: pure Brownian motion (stagnant fluid), laminar and turbulent shear flows. For the conditions of the experiments, the theory predicted that 1 in 10^4 to 1 in 10^6 of the particles arriving at the wall would bind permanently to the surface. When multiplied by the transport rate determined from CFD results, the experimentally observed rate of scaling is predicted correctly.

The results give a starting point to build a theory of silica colloid transport and deposition.

Wall roughness, which is enhanced as ridges of silica scale grow, is shown to enhance the scaling rate significantly. Further calculations and more experimental data are required to integrate roughness into the theory.

1. INTRODUCTION

Silica scaling, the deposition of colloidal silica in geothermal plant and wells, depends on both hydrodynamic and chemical conditions.

Experimental studies of colloidal silica transport in pipes suggest inertial effects dominate over diffusion in colloidal silica deposition [1, 2]. On the other hand, the theory of particle transport and deposition suggests that diffusion transport should dominate for these experimental conditions [2].

In this paper an attempt is made to resolve this contradiction by comparing previous experimental and new analytical and computational fluid dynamics (CFD) results and by analyzing the discrepancies.

1.1 Silica deposition on steel cylinders in crossflow

Silica deposition from natural geothermal brine onto cylinders in cross-flow was studied by Dunstall et al. [1]. The height of the silica ridges was found to vary significantly around the cylinder circumference. The maximum height of ~0.25 mm was reached at approximately 21° from the upstream stagnation point (Fig. 1). There was little to no deposition formed at the stagnation point, or on the downstream (wake) side of the cylinder. The height of the ridges is plotted in Fig. 2.

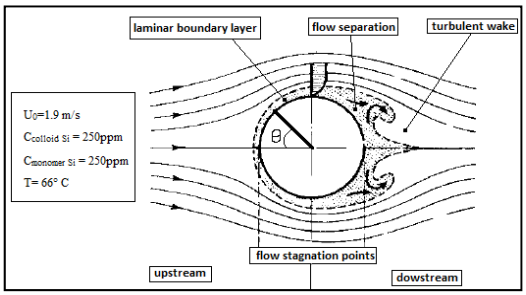

Figure 1: Flow around a circular cylinder [3] and conditions of the experiment [1]

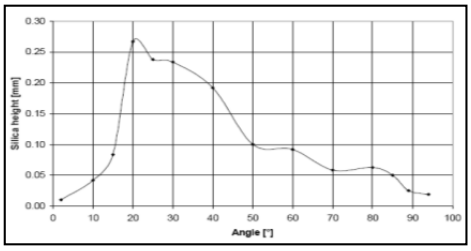

Figure 2: Experimental silica scale height over the circumference of a 25 mm diameter test cylinder; particle size 125nm; Re=1.07*10^5 [1]

The overall deposition rate increased as the average size of silica particles increased. This finding agrees with other experimental data on silica scaling [2].

The average scaling rate is calculated as a function of location on the cylinder circumference (Fig. 3) by dividing the total deposited mass by the experiment duration. The total deposition rate was calculated to be $2.2*10^{-9}$ kg/s per 1m of cylinder length from the curve in Fig. 3. In this calculation it is assumed that this curve describes the height of a continuous film of silica. In reality, though the curve follows the edges of the highest silica ridges, there are voids and pores between these ridges. Thus to find the real deposition rate the void fraction of the silica deposit is required. This is unknown but from inspection of the photographs in [1] it is estimated to be 0.25 with an uncertainty of ±50%. Taking this into account the total deposition rate averaged over the circumference of the cylinder is $(1.6\pm0.6)*10^{-9}$ kg/s per 1 m length, of the 25mm cylinder or $(4.2\pm1.6)*10^{-8}$ kg/s/m^2.

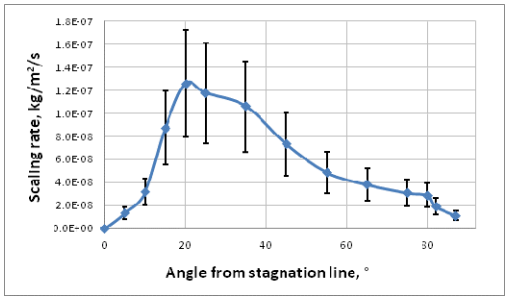

Figure 3: Silica scaling rate calculated from [1]

This experimental data is compared with theoretical speculations below.

1.2 General theory of particle transport

Uncharged particles suspended in a turbulent flow are transported to a stationary wall by two main mechanisms: diffusion and convection (the latter is sometimes called inertial transport). The flux of particles in the direction y normal to the wall for fully developed flow can be expressed as [4]:

$$j = -(D_B + D_T)\frac{\partial \overline{c}_p}{\partial y} + \overline{c}_p \overline{V}_{py}^{c} \qquad (1)$$

The first term on the right-hand side of Eq. 1 is the diffusion due to a gradient in the particle concentration and the second term represents convective transport emerging from particle inertia. The particle convective velocity in the y direction $\overline{V}_{py}^{c}$ is determined from the particle momentum equation which accounts for the gradients in turbulent intensity, shear induced lift and other external forces. In all calculations in this section, the particles are assumed not to interact with each other, or with the wall.

Numerical solutions of Eq. 1 and the corresponding particle momentum equation performed for the deposition on a smooth parallel surface allowed Guha [4] to find a relationship between non-dimensional deposition velocity V_{dep}^{+} and particle relaxation time τ_p^{+} (Fig. 4). The non-dimensional deposition velocity V_{dep}^{+} is the wall particle flux normalized by bulk concentration of particles c_p^0 and fluid friction velocity υ_0:

$$V_{dep}^{+} = j \Big/ c_p^0 \cdot \upsilon_0 , \qquad (2)$$

with $\upsilon_0 = \sqrt{\tau / \rho_l}$ determined from flow conditions (here τ denotes wall shear stress).

The dimensionless particle relaxation time is a measure of the particle's ability to deviate from fluid motion:

$$\tau_p^{+} = \frac{\rho_p d_p^2}{18\rho_l} \cdot \left(\frac{\upsilon_0}{\nu}\right)^2 ,$$

where ρ_p and ρ_l are particle and fluid densities correspondingly and ν the fluid viscosity.

Smaller particles (with short relaxation times) follow the fluid motion more closely than bigger particles, thus as they get closer to the wall they lose the y component of their convective velocity much faster than bigger particles.

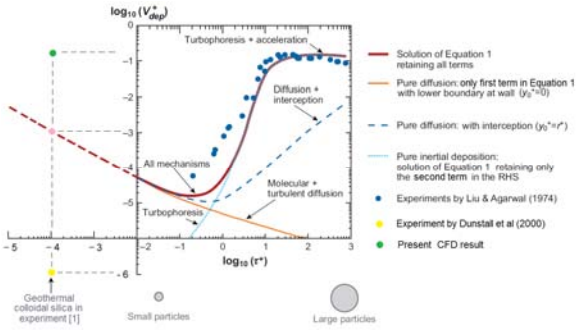

Figure 4: Classification of the particle transport mechanisms [4]

For very small particles this eventually leads to existence of a thin region close to the wall in which particle transport continues only by Brownian diffusion. This region is called the diffusion sublayer (see Fig. 6).

Interestingly, the dimensionless scaling velocity calculated for the conditions of the experiment [1] is $(1.4\pm0.5)\times10^{-6}$ which is about 3 orders of magnitude smaller than V_{dep}^{+} predicted by particle transport theory for the corresponding value of τ_p^{+} (yellow and pink circles in Fig. 4). This may indicate that in the experiment, colloidal silica deposition is retarded by the electrostatic particle–wall interactions discussed later in section 2.3.

Guha has also shown that particle deposition velocity is significantly affected by the roughness of the surface to which particles are transported (Fig. 5).

Real walls, having roughness elements protruding from their surface, experience higher mass transfer than ideal, perfectly smooth walls. In this particular case, particles need to be transported through the diffusion sublayer over distance equal to the theoretical sublayer thickness less the effective height of these roughness elements k_s. This increases transport of smaller particles for which this diffusion sublayer exists (see Fig.5 for $\log_{10}\tau_p^{+} \le 0$: silica colloids in geothermal brine have $\log_{10}\tau_p^{+} \approx -4$).

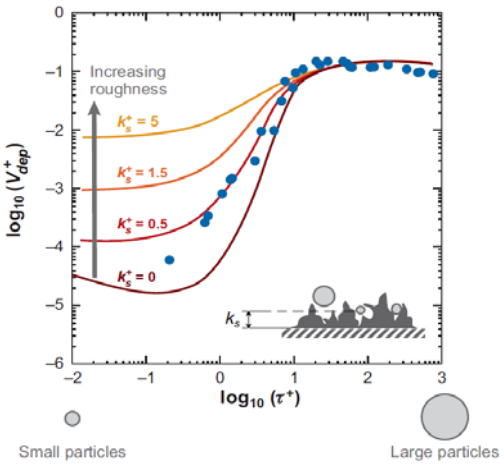

Figure 5: The effect of surface roughness on theoretical transport rate [4]

Here the dimensionless transport rate increases by almost 3 orders of magnitude when the effective height of roughness elements $k_s^+ = k_s \upsilon_0 / \nu$ increases from 0 to 5.

Finding k_s^+ values for the υ_0 (see Fig. 8, $\tau_{AVG} = 20Pa$) and ν characteristic of the experiments in [1] we can estimate the effect of roughness in silica scaling.

Thus, for new steel surfaces with $k_s = 0.05\,mm$ the dimensionless effective roughness height is $k_s^+ = 16$. Whereas if the effective height of the silica ridges is taken as $k_s \approx 0.12\,mm$ this value increases to $k_s^+ = 38$.

Comparing these values with the trends in Fig. 5 shows that the effect of surface roughness in silica deposition onto circular cylinder is significant for both of these cases.

In case of developed turbulent pipe flow, where the wall shear stress (is 1-5 Pa , the k_s^+ value for a new steel surface is about 6. This suggests the influence of roughness on silica deposition in pipes is also significant.

2. THEORETICAL STUDY OF SILICA TRANSPORT AND DEPOSITION ONTO CYLINDRICAL SURFACES

This section presents analytical and computational fluid dynamics (CFD) analysis of colloidal silica transport onto cylindrical collectors. For the former, a solution of the convection-diffusion equation from [5] was adopted to find the particle transport rate from a turbulent, isothermal suspension onto a smooth surface (section 2.1). Thus, no inertial effects or particle-particle/particle-wall interactions (i.e. no electrostatic forces) were considered in this case.

To evaluate the role of inertial particle transport the CFD simulations were performed (section 2.2). Again, no particle-particle or particle-wall forces were considered.

Both of these theoretical studies were conducted for hydrodynamic conditions identical to those of the experiment [1]. The analysis of the discrepancies between experimental and theoretical results provides valuable insight into the dominant mechanisms of particle transport.

Finally, to study effects of the inter-particle forces on the deposition process the interaction potentials were calculated for particle–particle and particle–wall interaction cases. These were then incorporated with analytical mass transfer calculations and the corresponding stability curves and coagulation/deposition rates obtained (section 2.3).

2.1 Analytical calculations

The diffusion problem [5] was considered with silica concentration $C_{Si} = 0$ on the cylinder wall and $C_{Si} = C_0 = 500\ ppm$ [1] in the bulk.

In an Eulerian frame the convection-diffusion equation can be used to describe molecular and particle solute transport (Eq. 3).

$$\frac{\partial C}{\partial t} + \upsilon_x \frac{\partial C}{\partial x} + \upsilon_y \frac{\partial C}{\partial y} + \upsilon_z \frac{\partial C}{\partial z} = D\left(\frac{\partial^2 C}{\partial x^2} + \frac{\partial^2 C}{\partial y^2} + \frac{\partial^2 C}{\partial z^2}\right) \qquad (3)$$

where D is either a molecular or Brownian diffusion coefficient of silicic acid molecules or colloidal silica particles respectively, in water. It is assumed that particles follow the flow streamlines perfectly. Thus, all inertial effects are neglected. These are considered in 2.2.

With a known velocity distribution $U = (\upsilon_x; \upsilon_y; \upsilon_z)$ and boundary conditions for C it is possible to find silica mass flux j to the surface by integrating Eq. 3.

Due to the close relation between the mass and momentum transfer processes, the concentration distribution near the solid surface has a layered structure similar to the flow velocity distribution. Thus, for the case of the turbulent flow over infinite plate (y=0) there are four regions with different mass diffusion patterns (Fig. 6). Far from the surface there is a zone of developed turbulence (region I) where both average velocity and concentration have constant values ($C_I = C_0$ for $y > d$). Closer to the surface, in the turbulent boundary layer (region II), the average velocity, and so the concentration, decrease slowly according to a logarithmic law (Eq. 4):

$$C_{II} = \frac{j}{\beta \upsilon_0} \ln \frac{y}{d} + C_0 \quad \text{for} \quad \delta_0 < y < d\,, \qquad (4)$$

where β is a constant numerical coefficient.

Further, with an assumption of gradual decay of turbulence within the viscous sublayer [5], over the region III $(\delta_0 > y > \delta)$ mass transport by residual turbulent pulsations is still stronger than mass transport by molecular/Brownian diffusion. It can be shown that solute (monomeric or colloidal Si in this case) distribution in this region is given by Eq. 5:

$$C_{III} = \frac{j\delta}{D} + \frac{j\delta_0^3}{3\gamma\upsilon_0}\left(\frac{1}{\delta^3} - \frac{1}{y^3}\right) \qquad (5)$$

where γ is a certain numerical coefficient.

Only in the innermost part of the viscous sublayer (region IV), at $y < \delta$, does the molecular (Brownian) diffusion mechanism prevail over the turbulent, so here (Eq. 6):

$$j = D\frac{\partial C}{\partial y} \quad \text{and} \quad C_{IV} = \frac{j}{D}(y - a) \qquad (6)$$

where a is an average particle radius in case of colloidal silica transport and a=0 for the monomeric silica.

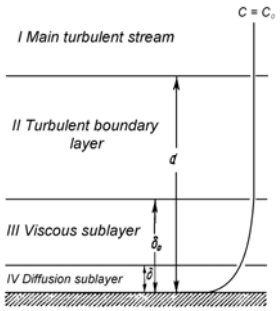

Figure 6: Structure of the diffusion boundary layer [5]

Equating the expressions for C_{III} and C_{IV} at $y = \delta$ gives the flux (Eq. 7):

$$j = \frac{DC_0}{-\frac{D}{\beta\nu_0}\ln\frac{\delta_0}{d} + \frac{\delta_0^3 D}{3\gamma\upsilon_0}\left(\frac{1}{\delta^3} - \frac{1}{\delta_0^3}\right) + \delta} \quad (7)$$

The height of the diffusion boundary layer according to [5] is (Eq. 8):

$$\delta = \left(\frac{\delta_0^3 D}{\gamma\upsilon_0}\right)^{1/4} = \frac{\delta_0}{Sc^{1/4}\sqrt[4]{10\,\gamma}} \sim \frac{10^{3/4}\nu}{Sc^{1/4}\sqrt[4]{10\,\gamma\,\upsilon_0}}, \quad (8)$$

where $Sc = \frac{\nu}{D}$ - dimensionless Schmidt number, the ratio of momentum diffusion (viscosity) to mass diffusion.

For high values of the Schmidt number (*e.g. Sc~10^3)* the expression for mass flux simplifies to (Eq. 9):

$$j \approx \frac{DC_0}{\delta\left[\frac{4}{3} - \frac{\sqrt[4]{\gamma}}{(10\cdot Sc)^{3/4}\beta}\ln\frac{\delta_0}{d}\right]} \quad (9)$$

and $\delta \sim 1/6\ \delta_0$ in this case. The unknown numerical constants β and γ were found experimentally to be of order unity and thus it can be shown that the second term in the denominator is substantially smaller than the first, and can be neglected to simplify Eq.9 to Eq.10:

$$j \approx \frac{DC_0}{\frac{4}{3}\delta} = \frac{C_0\upsilon_o}{\alpha Sc^{3/4}}, \text{ where } \alpha = \frac{4}{3}10^{3/4} \quad (10)$$

If the bulk silica concentration, diffusion coefficient (molecular for dissolved Si and Brownian for the colloidal) and thickness of the boundary layer are known, it is possible to find the maximum realizable (i.e. not limited by the surface reaction rate) diffusion flux toward any surface by integrating Eq. 10 over its area.

In the case of diffusion to a circular cylinder in a crossflow, when the boundary layer is laminar over the upstream part of its circumference and becomes turbulent downstream from the separation line, the total diffusion flux to the cylinder surface can be shown [5] to be (Eq. 11):

$$J = \frac{196}{360}\frac{\pi L^2}{4}\frac{DC_0}{Sc^{1/3}}\left(\frac{U_0}{\nu L}\right)^{1/2} + \frac{164}{360}\frac{\pi L^2}{4}\frac{\sqrt{K_f}U_0C_0}{Sc^{3/4}} \quad (11)$$

where U_0 is the velocity of undisturbed flow far away from the cylinder and $K_f \approx \frac{0.27}{\mathrm{Re}^{0.1}}$ the drag coefficient.

The diffusion transport rate calculated from Eq. 11 and corresponding experimental results are shown in Table 1.

The monomeric (or direct) silica deposition was found experimentally to be very slow [2, 6, 7] and not responsible for the scale build-up. So, the calculated transport rate of the monomeric silica being higher by two orders of magnitude than the experimentally observed deposition rate suggests that this mechanism is limited by the surface reaction rate of monomeric silica attachment to the wall surface. The distribution of dissolved silicic acid in the flow thus must be near uniform (i.e. same at the wall surface and in the bulk flow) unless there is some non-transport reason for the concentration to vary with location (e.g. a thermal gradient).

The colloidal silica transport rate obtained in the analytical calculations is within the uncertainty interval of the mean experimental value. Interestingly, Eq. 11 predicts transport rate towards the downstream part of the cylinder to be higher than that to the upstream part. This correlates with the assumption made about the boundary layer state, but is contrary to the scale distribution observed experimentally.

It is possible that inertial transport, not included in this analytical model, is responsible for the observed distribution of scale. To investigate the role of inertial mechanisms of particles transport, CFD simulations of particle transport were performed.

2.2 CFD calculations

ANSYS Fluent software, was used to model the transport of the colloidal particles, using Lagrangian particle tracking and allowing both convective diffusion and inertial effects to be modelled simultaneously. The corresponding 2D computational domain is outlined in Fig. 7. It comprised 180,000 mesh nodes representing a rectangular region of flow (250x125 mm) with a circular cutout (25mm in diameter) in the middle. The circle represented the surface of the cylinder, so the no-slip condition for the flow and an

Table 1: Comparison of the experimental, analytical and simulation results

		Total per 1 m length of a cylinder, kg/s	Average per unit area, kg/s/m^2	Dimensionless, @ $\tau = 20Pa$
Experimental deposition rate		$1.6\pm0.6\times10^{-9}$	$4.2\pm1.6\times10^{-8}$	$1.2\pm0.5\times10^{-6}$
Analytical transport rate	monomeric Si	1.4×10^{-7}	1.7×10^{-6}	4.8×10^{-5}
	colloidal Si	2.9×10^{-9}	3.7×10^{-8}	1×10^{-6}
CFD transport rate of colloidal Si		4.7×10^{-4}	1.2×10^{-2}	3.4×10^{-1}
Theoretical transport rate towards a smooth parallel wall from Fig.4				1×10^{-3}

ideal sink for the particles were imposed on it. The water entered the domain through the velocity inlet boundary condition with average velocity of 1.9 m/s and temperature 66°C. Surface type particle injection was specified at the same boundary. Total colloidal silica mass flow rate was set to 0.098 kg/s. This corresponds to 250 ppm of colloidal silica suspended in the flow.

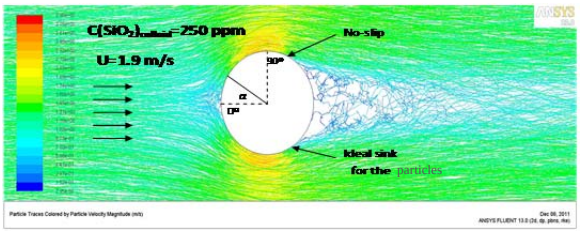

Figure 7: Outline of the computational domain

The problem was solved in two steps. First, a converged steady state solution for the flow equations was obtained. A convergence criterion of 10^{-6} for the scaled residual of the continuity equation was used. The solution was verified by comparing calculated and experimentally measured distribution of the pressure coefficient along the cylinder circumference. Less than 20 % difference was found.

In the second step, a discrete phase model was enabled and transient calculations of the coupled particle-flow dynamics were performed. On average, 10 seconds of the flow time were computed. In order to record the particle mass flux to the cylinder surface, the accretion model was used [8].

The overall transport rate of colloidal silica obtained in this way is given in Table 1, while its distribution over the cylinder circumference is illustrated in Fig. 8.

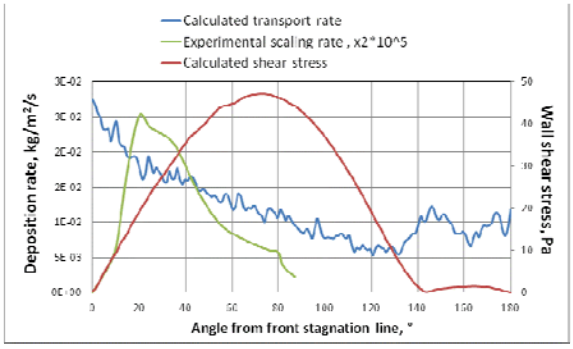

Figure 8: Comparison of CFD and experimental results

The rate of transport of colloidal silica in these CFD simulations is five orders of magnitude higher than the experimentally measured deposition rate and the rate computed from the analytical model in the previous section. This discrepancy may suggest that the scale growth caused by colloidal silica is limited by its attachment to the surface (chemical bonding) which is intimately related to particle-wall interaction (electrostatic force).

Both analytical and CFD model omit attachment and electrostatic effects, yet the CFD predicts a higher rate of transport than the analytical model and the theory in Fig.4. Some hypotheses which may explain this discrepancy are:

- the CFD model's better representation of the flow field around the cylinder (than the one used in derivation of Eq. 11) affects the transport;
- the inertial transport of particles, which is not accounted for in the analytical model, but is present in the CFD, is dominant;
- the curvature of the cylinder surface and the Saffman lift forces, which are present in the CFD but not in the theory used to generate Fig. 4 enhance the transport of colloidal silica to the surface.

The shapes of the experimental and predicted deposition profiles are different, with the simulated colloid transport rate peaking at the stagnation line on the front of the cylinder, but the observed scaling rate peaking at 21°. However, the colloid transport rate and scaling rate are not the same parameter and cannot be directly compared. The observed scaling rate may be explained by combining the predicted transport rate with the attachment probability, i.e. the fraction of particles that reach the surface and actually bond and remain on the surface, all others remaining in the flow. This fraction is estimated based on the DLVO theory of charged colloidal particles interaction in the next section.

To summarise the findings so far, particles can travel to the surface by diffusion or inertial transport. The diffusion transport rate of particles (calculated from the analytical model) is of the same order of magnitude as the experimentally observed deposition rate. The inertial transport rate calculated from the CFD model is several orders of magnitude higher than the experimentally observed deposition rate. Both analytical and CFD models exclude particle-particle and particle-wall interactions. Theory and experiment may be reconciled with the experimental observations if, due to those interactions, only a small fraction of the particles arriving at the surface bind to it. To investigate this, particle-particle and particle-wall interactions are considered in the next section.

2.3 Theoretical model incorporating electrostatic and hydrodynamic effects

Being in continuous Brownian motion in addition to the motion induced by the suspending fluid, colloidal particles experience numerous mutual collisions and collisions with stationary walls. In the absence of any limiting factors each of these collisions would results in close contact between particles followed by chemical bonding and agglomeration (or attachment to the surface). This process is called fast, or rapid, aggregation as it results in all colloidal particles being separated from the solution as aggregate in a matter of minutes.

However, depending on the solution pH, silica colloids can carry uncompensated surface charge due to ionization of the surface silanol groups. The presence of charge of the same sign on all particles, and on wall surfaces covered with amorphous silica, results in an electrostatic potential barrier which the particles need to overcome to form the bond. Due to this so called electrostatic stabilization, not all collisions of the particles lead to aggregation or particle attachment to the surface. This process is called slow aggregation. Under the right conditions charge stabilized colloidal systems can be stable for very long periods of time (years).

The potential barrier between charged particles is usually so high (in terms of potential energy) and wide (in terms of distance of approach) that individual particles are unable to pass it in one attempt – they lose all kinetic energy obtained in separate Brownian projections well before they clear the potential barrier, due to friction with surrounding liquid (viscous interaction). The particles overcome the barrier in a sequence of Brownian collisions rather than in one step.

This allows the effect of the interparticle forces to be treated as an additional diffusion process [9]. In this case the corresponding particle flux can be expressed as (Eq. 12):

$$J_{DLVO} = \frac{n}{B}\frac{dV_t}{dr}, \qquad (12)$$

where n is local particle concentration, B is the friction factor and V_t is total interaction potential, which equal to sum of the attractive and repulsive potentials calculated from DLVO theory [2, 10].

For the simplest case of a stagnant colloidal suspension, when total particle flux (towards each other) is determined only by Brownian motion and electrostatic potential yields the following for the stability value [9] (Eq. 13):

$$W = \frac{Number\ of\ \ particle\ collisions}{Number\ of\ collisions\ resulting\ in\ coagulation} = 2\int_2^\infty \exp\left(\frac{V_t}{kT}\right)\frac{ds}{s^2} \qquad (13)$$

where $s=r/a$ is a non-dimensional distance between particles (or particle and wall), r is centre-to-centre (or centre-to-wall) distance, and a is particle radius.

Stability curves calculated with this equation for two particle sizes are presented in Fig. 9 (broken lines). It shows that colloid stability W decreases with increasing ionic strength of the solution I (concentration of dissolved salts) and with decreasing particle size d. It can be seen that in silica sols with sufficiently low ionic content only 1 in 10^{10} collisions result in particle coagulation.

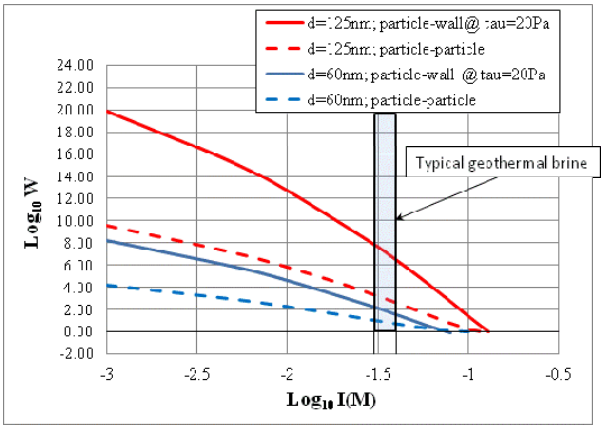

Figure 9: Stability curves for colloidal silica sols

The case of flowing colloidal solution is of more practical interest. The rate of particle collisions can be much higher than in the stagnant case due to the presence of velocity gradients and turbulent pulsations. Thus, Levich gives the following expressions for the number of particle-particle collisions per second [5]:

- Brownian encounters $N_{Brw} = 8\pi D d n_0$
- Gradient encounters $N_{Grad} = \frac{32}{3} n_0^2 d^3 G$
- Turbulent encounters $N_{Turb} = n_0^2 d^3 \upsilon \frac{\mathrm{Re}^{3/2}}{L^2}$

where D is the particle diffusion coefficient, d its diameter, n_o the number of particles per unit volume, G the velocity gradient, Re the Reynolds number, ν the kinematic viscosity and L the characteristic length.

Calculating these numbers for the conditions of the experiment [1] we find (Fig. 10) that the number of encounters due to the velocity gradients is higher by several orders of magnitude than those due to Brownian motion. Here the broken blue line is obtained for the velocity gradient $G=5*10^6\ s^{-1}$. This value corresponds to the maximum shear stress in turbulent flow around a cylinder (Fig. 8). Also, the difference in slopes of the curves in Fig. 10 shows a slower decay of gradient-induced collision rate with increasing particle size than for the Brownian collisions.

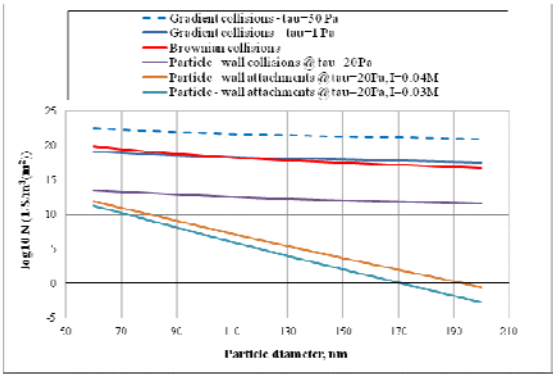

Figure 10: Rates of idealized collision processes

Unfortunately, an attempt to calculate the aggregative stability of colloidal system with gradient or turbulent collisions included faces significant theoretical difficulties. The steady-state convection-diffusion equation with electrostatic particle interaction term must be resolved on the particle size length scale to find the total number of other particles reaching the surface of the selected centre particle. In this case finding the solution cannot be simplified by using the boundary layer approach (as was done in finding mass flux to a flat wall, Eq. 10). The thickness of the diffusion boundary layer present on the particle surface is comparable with particle size. Thus (in essence inertial) effects of the particle's relative motion due to the velocity gradients in mean flow and turbulent pulsations may significantly affect the mass transfer rate. Presumably, this problem can be tackled numerically.

On the other hand it is relatively straightforward to include the additional particle flux due to the electrostatic interaction between particles into the problem of particle transport towards a smooth wall.

For this we assume that the target surface caries uniform charge of the same sign and magnitude as SiO_2 colloids suspended in the flow. Physically this corresponds to the ideally smooth amorphous silica surface. Next, we assume that the region of significant inter-particle interaction lies entirely within the diffusion boundary layer. This is true for the conditions of the experiment [1] (as diffusion boundary layer height is 300-2000nm, whereas interaction potential can be neglected at separation distances above 50 nm). This assumption would be violated only for a very fast flow (shear velocity ~0.5 – 1 m/s).

This last assumption allows us to express the particle concentration distribution in the diffusion boundary layer (region IV in Fig. 6) as (Eq. 14):

$$c_{IV} = c(\delta) - \frac{j_s}{D}\int_\delta^a \exp \bar{V} dr\,, \qquad (14)$$

where $c(\delta)$ is particle concentration at the edge of the diffusion boundary layer $y=\delta$, subscript s is for the "slow" particle flux – retarded by the interaction forces. Using the condition of concentration continuity at $y=\delta$ we can find

j_S by comparing equations 14 and 10 (for c_{III} expressed through c_{II}). Simplifying the result the same way as for Eq. 10 we arrive at (Eq. 15):

$$j_S = \frac{Dn_0}{\int_{\delta}^{a} \exp\bar{V} dr + \delta/3} \quad (15)$$

where δ is the diffusion boundary layer thickness (Eq. 8), a is particle radius, $\bar{V} = \frac{V}{kT}$ is the - ratio of electrostatic interaction potential and molecular thermal energy.

Calculating ratio of j_f (determined by Eq. 14) and j_S Eq. 15) we get the stability of the colloids to deposition onto smooth surface (Eq. 16):

$$W = \frac{3}{4} \frac{\int_{\infty}^{a} \exp\bar{V} dr}{\delta - a} \quad (16)$$

Fig. 11 illustrates solutions of the Eq. 16 for three particle sizes and two solution ionic strengths. Stability curves from Eq. 16 also shown in Fig. 9 for comparison with the particle-particle interaction case. Similarly to particle-particle collisions, the ratio of successful particle-wall collisions decreases with increasing particle size and decreasing ionic strength.

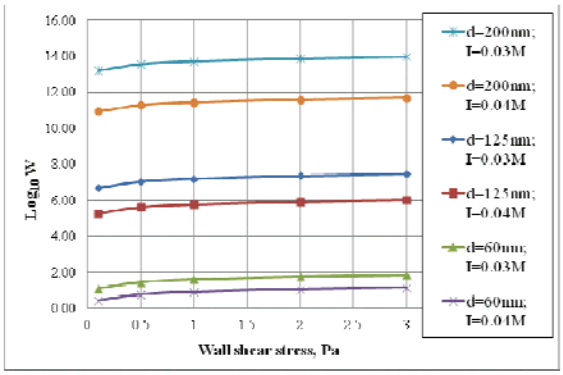

Figure 11: Colloidal silica stability in smooth surface scaling

The idealized particle-wall collisions modeled here are less likely to result in binding than particle-particle collisions (Fig. 9). This agrees with the fact that the electrostatic potential is twice as high for particle-wall interactions than for particle-particle interactions, but contradicts the experimentally observed behavior of such systems, that particle deposition onto stationary walls has a higher or similar rate to particle aggregation in the bulk. Experiments also show that this rate increases with increasing particle size.

The rate of bonding in the particle-wall collisions has a weak dependence on the shear stress (Fig. 11). It is worth mentioning that this dependence is mostly caused by the variation of the "fast" surface particle flux (Eq. 10) with diffusion boundary layer thickness. Whereas, its "slow" counterpart (Eq. 15) was found to be almost independent of the flow conditions. The first term in the denominator of the Eq. 15 is significantly higher than the second. This means that, in this particular idealized case, mass transfer to the wall is more severely limited by the potential barrier than by the convection-diffusion transport. The transport of particles can limit the deposition rate in case of very slow flow velocities, when the convective diffusion rate is very small. Also, the transport of particles to the surface may be so fast that the thickness of the boundary layer can become comparable with characteristic length of the inter-particle interactions. This, as well as surface roughness, requires a more complex model than that presented here.

3. DISCUSSION

Stability values of the two marginal collision scenarios considered in Section 2.3 can be used to assess particle attachment probability in silica scaling process.

Surfaces of powerplant equipment can rarely be considered smooth. Their inherent roughness affects particle transport and electrostatic interaction. If they contain roughness elements of micrometer scale with varying radii of curvature. If assumed to be coated with a monolayer of silica, they will have heterogeneous distributions of surface charge.

This heterogeneity is even higher when the surface is covered with a layer of colloidal particles. Though areas of high curvature near particle contact points become smoothed by monomeric silica deposition, the average effective surface curvature remains at the same order of magnitude as the particle size. New particles arriving at the wall will interact with those particles which arrived and bonded earlier. We hypothesise that the stability of such "particle - rough wall" collisions is between the corresponding values for the "particle-particle" and "particle-smooth wall" cases presented in Fig. 9.

For the hydrodynamic and chemical conditions of the experiment [1] this gives stability value $10^4 < W < 10^6$ i.e. 1 in 10^4 to 1 in 10^6 particles arriving at the wall will bind, the rest (the majority) will return to the flow. Other calculations presented in Section 2.3 predict that W will increase with increasing particle size and decreasing wall shear stress (or effectively convective transport rate).

The former effect is expected as higher particle diameter means lower curvature and thus a higher interaction potential barrier. The latter effect is more complex. The fraction of particles that pass through the potential barrier may be affected by the variations in particle kinetic energy distribution (caused by convection and particle inertia). With a lack of evidence to the contrary it is assumed, for now, that W is determined solely by the physicochemical properties of the colloidal system. This allows for the silica scaling process to be treated like a chemical reaction of the first order by concentration (flux) of particles on the reaction surface:

$$[Scaling\ rate] = k*[Transport\ rate]$$

where $k = 1/W$ is particle attachment probability.

The particle transport rate value obtained in the CFD simulations (Fig. 12, green circle) can now be converted into expected scaling rate:

$$[3.4\times10^{-1}]*10^{-5} = 3.4\times10^{-6}$$

which is the same order of magnitude as the experimental scaling rate (yellow circle).

However, the CFD transport rate may be overestimated as a smooth surface was assumed. It seems unlikely it will be even higher than the transport rate in an inertia dominated regime $(\log_{10}\tau_p^+ \geq 1)$.

Extrapolating the trend that increasing surface roughness raises the transport rate, the green circle in Fig. 12 is close to the expected value of transport rate in experiment [1] with fully developed roughness.

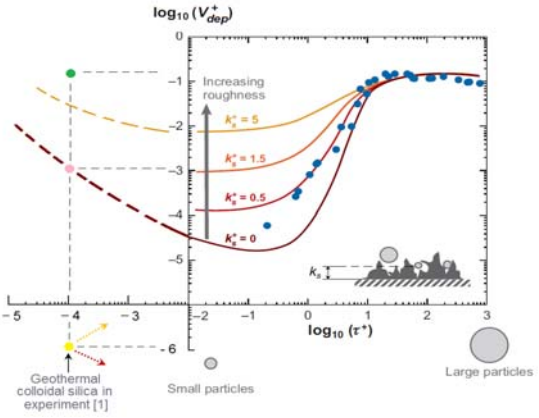

Figure 12: Theoretical and experimental trends in the silica scaling

The difference in theoretical predictions and experimental observations of the scaling rate behavior with increasing particle size is illustrated schematically in Fig. 12. Experimental data (yellow broken arrow) shows that the scaling rate increases with particle size. Meanwhile, theoretical results (red broken arrow) suggest that both attachment probability and transport rate decrease with increasing particle size.

It is hypothesized that in this range of particle sizes, increasing particle inertia, though it has insignificant effect on convection normal to the wall, intensifies tangential (parallel to the wall) convection onto roughness elements protruding from the wall.

This argument also may explain the difference observed (Fig. 8) between the spatial distributions of scale on the cylinder in experiment and theory. Higher scaling rate may be expected at locations with higher wall shear stress. First, the thickness of the diffusion boundary layer is smaller here which makes the effect of existing surface roughness higher. Second, at the locations with higher wall shear stress particles have higher tangential velocity and thus higher inertial deposition rate in this direction.

The wall shear stress distribution in Fig. 8 was calculated for a smooth cylinder. For a rough cylinder its maximum will probably shift towards the front. This is because roughness elements decelerate the flow and render near wall velocity distribution more uniform downstream from where they are located. Thus, the observed scale distribution around the cylinder may coincide with real wall shear stress distribution.

4. CONCLUSIONS

The comparison of experimental and new theoretical results on silica scale formation found the following:

1. The scaling rate may be expressed as a product of the rate of transport of silica particles to the surface and the probability of their permanent attachment to it.
2. Calculations of inertial and diffusional transport of particles without electrostatic interactions predict a transport rate several orders of magnitude higher than the experimentally observed scaling rate.
3. Increasing surface roughness significantly increases (by orders of magnitude) the particle transport rate to the surface. Surface roughness will increase as particles bond to the surface. Understanding the role of surface roughness may explain the effect of particle size effect on silica scaling.
4. The particle attachment probability can be determined based on the DLVO theory of colloidal particle interactions.
5. Such calculations show that attachment probability decreases with increasing particle size and decreasing ionic strength of the solution
6. For the conditions of the silica scaling experiment [1] this probability was argued to be $10^{-4}<W^{-1}<10^{-6}$ which when multiplied by the computed transport rate (taking into account both diffusional and inertial transport) predicts to within an order of magnitude the experimentally observed scaling rate. Roughness effects may explain the remaining discrepancy, but this must be investigated further.
7. The CFD transport rates may vary with further refinement of the mesh in the near-wall region.
8. Further work is required to integrate surface roughness into the model.

ACKNOWLEDGEMENTS

We wish to thank Mighty River Power for supporting this study and in particular Michael Rock, Simon Addison and Jeff Winick for technical advice.

REFERENCES

1. Dunstall M., Zipfel H. and Brown K. L.: *The onset of silica scaling around circular cylinders*, World Geothermal Congress, Kyushu-Tohoku, Japan, pp. 3045-3050. (2000).

2. Kokhanenko P., Masuri S., Jermy M., Sellier M. and Brown K.: *Hydrodynamics and electrochemistry of silica scaling*, 34th New Zealand Geothermal Workshop, Auckland, New Zealand, (2012).

3. Schlichting, H.. Boundary-Layer Theory. *McGraw-Hill Book Co. New York.* (1979)

4. Guha A.: Transport and Deposition of Particles in Turbulent and Laminar Flow, Annu. Rev. Fluid Mech. 40:311–41. (2008).

5. Levich V., *Physicochemical hydrodynamics*: Prentice-Hall, Inc., (1962).

6. Iler R. K., *The chemistry of silica: solubility, polymerization, colloid and surface properties, and biochemistry*: Wiley, (1979).

7. O. Weres, et al.: Kinetics of silica polymerization, Journal of Colloid and Interface Science, vol. 84, pp. 379-402. (1981).

8. ANSYS Fluent Documentation, Theory Guide

9. Hunter R. J., *Introduction to modern colloid science*, Oxford University Press, Oxford, (1993).

10. Adamczyk Z., Weronski P., *Application of the DLVO theory for particle deposition problems.* Advances in Colloid and Interface Science 83, 137-226 (1999).